



OPEN

External Cesium-137 doses to humans from soil influenced by the Fukushima and Chernobyl nuclear power plants accidents: a comparative study

Ka-Ming Wai^{1,2}✉, Dragana Krstic³, Dragoslav Nikezic³, Tang-Huang Lin⁴ & Peter K. N. Yu⁵✉

External exposure to gamma-photon irradiation from soil contamination due to nuclear power plant (NPP) accidents has significant contribution to human radiation exposure in the proximity of the NPP. Detailed absorbed doses in human organs are rarely reported in the literature. We applied the **Monte Carlo Neutron Particle (MCNP)** transport code to calculate and compare the absorbed doses in different human organs. The absorbed doses by gamma-photon radiation were from cesium-137 (¹³⁷Cs) in soil contaminated by the two major NPP accidents. More serious and wide-spread impacts of the Chernobyl NPP accident on soil contamination in Ukraine, Belarus, Russia and countries as far as Sweden and Greece were due to the inland location, radiative plume transport pathway and high ¹³⁷Cs emission strength (9 times the Fukushima emission). Based on our MCNP calculations, the largest absorbed dose was found in skin. The maximum calculated external ¹³⁷Cs annual effective dose received from the Chernobyl accident was 10 times higher relative to the Fukushima accident. Our calculated effective doses at various influenced areas were comparable to those available in the literature. The calculated annual effective doses at areas near the Fukushima and Chernobyl NPPs exceeded the ICRP recommendation of 1 mSv yr⁻¹.

The Fukushima and Chernobyl nuclear power plant (FNPP and CNPP) accidents are the two largest sources of anthropogenic radionuclides released into the environment in recent years. The former was triggered by the Tohoku-earthquake induced tsunami on 11 March 2011, which caused damage of the main cooling systems and left the reactors overheated and led to hydrogen gas explosions. The explosions resulted in damaging of the FNPP buildings. The latter accident was initiated by an operating error on 26 April 1986 which caused xenon poisoning (and its reaction) of the Unit 4 reactor of the CNPP. It led to thermal destruction of the reactor and caused ignition of the graphite moderators. Following about one-quarter of the total radioactive materials released during the early stages of the accident, a second stage of the continuous release was due to the graphite fire¹. The major difference between the two accidents is that the release of the FNPP is mainly chemical in nature (gas-phase only) but the CNPP released part of the core reactor inventory. Due to the adverse impacts of the CNPP accident to humans, a large-scale human evacuation from the CNPP was required (https://www-pub.iaea.org/MTCD/Publications/PDF/te_1240_prn.pdf) and resulted in a land use change. The land use change before and after the CNPP accident was detected through satellite observations (Supplementary Materials S1).

Specifically, cesium-137 (¹³⁷Cs) with a half-life of 30.1 years derived from the NPP accidents has been intensively studied due to its significant adverse impacts on the environment through atmospheric deposition. The ¹³⁷Cs deposition is depended on various factors such as strength/mode of accidental release, atmospheric transport pathways and plume inception in areas with local precipitation. Previous relevant studies have described the

¹Department of Civil and Environmental Engineering, College of Engineering, Shantou University, Shantou, China.

²Intelligent Manufacturing Key Laboratory of Ministry of Education, Shantou University, Shantou, China. ³Faculty of Science, University of Kragujevac, R. Domanovica 12, Kragujevac, 34000, Serbia. ⁴Center for Space and Remote Sensing Research, National Central University, Taoyuan City, Taiwan. ⁵Department of Physics, City University of Hong Kong, Hong Kong SAR, China. ✉e-mail: jmwei@stu.edu.cn; peter.yu@cityu.edu.hk

long-range transport of ^{137}Cs from the CNPP in Ukraine affected European countries more than 1000 km away^{1–4}. Similarly, local/regional and cross-Pacific transport of ^{137}Cs and its downwind impacts from the FNPP accident has also been studied^{5–10}. Other studies reported the measurements of ^{137}Cs deposition after the atmospheric transport^{11–24}.

The external radiation doses in the human body irradiated by gamma photons from ^{137}Cs deposited in soil are of particular concern. Recent studies related to the FNPP accident for areas within the Fukushima prefecture, Japan have been undertaken^{25,26}. Similar investigations at Bryansk, the most impacted areas by the CNPP accident in Russia, have been reported^{27–29}. A study was carried out which focused on recent external doses in Minsk and Gomel, Belarus and Chernobyl, Ukraine in 2012³⁰. It reported the estimated effective doses around CNPP to be still over the public dose limit of 1 mSv yr^{-1} recommended by the ICRP³¹ 26 years after the accident. The above studies were mainly undertaken at different local/regional-scale areas. A large-scale or country-scale comparative study on the soil distribution of ^{137}Cs and associated absorbed doses in the human organs between different impacted areas are rarely available in the literature, despite the fact that the determination of organ doses is important for cancer risk assessment^{32,33}. The organ doses estimation has been conducted for populations near nuclear facilities³⁴.

In the current study, we first summarized, compared and explained the literature values of the ^{137}Cs activity concentrations in soil measured in various areas influenced by the NPP fallouts. The external gamma-photon absorbed doses in different human organs due to derived ^{137}Cs concentrations in contaminated soil in these areas were then calculated by the MCNP code. The calculated human organ doses (in more than ten organs) around the NPPs were then compared, which is the novelty of our study. Finally, we evaluated our calculated annual effective doses with the reported values available in the literature for the FNPP and CNPP accidents. Given the available soil concentrations of ^{137}Cs , our study provided a method to calculate the annual effective doses at various areas where there were no estimates on effective doses available. The CNPP accident results were considered for the time immediately after the accident in order to have a meaningful comparison.

Results and discussion

Comparison of ^{137}Cs soil concentrations due to the NPP accidents. Table 1 summarizes the literature values of ^{137}Cs concentrations (kBq kg^{-1}) in soil at various locations influenced by the FNPP and CNPP accidents. All the data reported here for CNPP accident are the values as in 1986. Not only the source-receptor distance, but also the meteorological setting for the radiative plume transport and soil property could affect the soil concentrations at a specific location. For the Fukushima event, the maximum soil concentration (66.7 kBq kg^{-1}) was found in Minamisohma city 15 km from the NPP. Cities locating relatively far away from the NPP ($>50\text{ km}$) had smaller contamination of order of 10 kBq kg^{-1} or less. The data of ^{137}Cs soil concentrations influenced by the CNPP accident were difficult to obtain since the available data in the literature were reported in kBq m^{-2} . Extremely high soil concentration ($>250\text{ kBq kg}^{-1}$) was found less than 30 km from the CNPP^{14,18}. Within 100 km from the CNPP, the concentration was more than 20 kBq kg^{-1} but the contamination pattern was highly irregular and anisotropic. Total areas of 7200 and 116000 km^2 with maximum concentrations of 23 and 2.8 kBq kg^{-1} were located in Belarus, Russia and Ukraine¹⁶. For the far field, Sweden, Austria and Greece showed abnormally high soil contamination¹⁴, attributed to the long-range transport of radiative plume. It was noted that the ^{137}Cs deposition on Sweden was highly uneven¹¹ and reference therein, and therefore the concentrations at both lower and higher sides were presented in Table 1. The uneven deposition was a result of changing meteorological conditions during the dispersion of released materials¹⁴.

While some FNPP fallout occurred on the Japan landmass, the majority (80%) was on the northern Pacific Ocean along with the prevailing westerly^{8,35,36} since the FNPP is located at the coastline. Therefore the influences of the radiative plumes to other countries such as those in Northern America and Europe were small^{7–10}. On the contrary, the CNPP was located well within the European continent. The large initial release height ($>1\text{ km}$ above ground) of the radiative plumes due to explosions at the CNPP and convective updraft of the plumes during long-range transport were the major reasons of the high ^{137}Cs deposition to areas in northern and southern European countries located $>1000\text{ km}$ from the CNPP^{1–3,37,38}. The large differences in soil contamination for the two accidents were also due to the large differences in atmospheric release of radionuclides ^{137}Cs , which were in the range of 74–98 PBq for the CNPP^{39–41} and 12–17 PBq for the FNPP^{7,42–44}.

Calculated equivalent dose in organs and effective dose in areas influenced by the NPP accidents.

The MCNP modeling results calculated for equivalent doses in various organs of the mathematical phantom are given in Table 2. Skin and bone surface, and thyroid received the largest and smallest equivalent doses, respectively. Figure 1 shows the calculated annual external effective doses due to the ^{137}Cs derived gamma photons irradiation calculated for various areas with contaminated soil influenced by the FNPP and CNPP accidents. The calculated annual effective doses for the CNPP accident were evaluated immediately after the accident as described above to have a meaningful comparison with the FNPP accident. The calculated maximum annual effective dose in areas affected by the CNPP accident was about 10 times higher compared with that in areas affected by the FNPP accident. Similarly, the near-field areas (in Ukraine, Belarus and Russia) received higher effective doses from the CNPP accident than those from the FNPP. Interestingly, the people habitat in Greece ($\sim 1400\text{ km}$ from the CNPP) received comparable effective dose as people in the Nishi-Shirakawa County, Japan located 85 km away from the FNPP. Even the lowest effective doses ($0.01\text{--}0.02\text{ mSv yr}^{-1}$) calculated for Austria and Sweden for the current study, which were affected by the CNPP accident, were still several times higher than the background effective doses received in South Asian countries^{45,46}.

For the accident in Japan, our result of calculated annual effective dose of 0.9 mSv yr^{-1} obtained for Fukushima City (Fig. 1) was well comparable to the external ^{137}Cs dose assessment for the same City (0.5 mSv yr^{-1}) by Yoshida and Suzuki²⁵. Taira *et al.*²⁶ reported the total external effective doses at the same location, which ranged from 2.2

| Location | Distance from NPP (km) | Concentration (kBq kg ⁻¹) ^a | References |
|--|------------------------|--|---|
| FNPP accident | | | |
| Namie town | 8 | 33.1 | ²³ (Table 1), ²⁴ (Table S1) |
| Minamisohma city | 15 | 66.7 | ²³ (Table 1), ²⁴ (Table S1) |
| J Village | 20 | 9.4 | ²⁰ (Table 1) |
| Motomiya city | 50 | 8.4 | ²³ (Table 1), ²⁴ (Table S1) |
| Fukushima city | 60 | 15.8 | ²¹ (Fig. 4), ²² (Fig. 1), ²³ (Table 1), ²⁴ (Table S1) |
| Koriyama city | 60 | 11.4 | ²² (Fig. 1), ²³ (Table 2), ²⁴ (Table S1) |
| Nishi-Shirakawa county | 85 | 1.6 | ²² (Fig. 1), ²⁴ (Table S1) |
| CNPP accident | | | |
| Chistogalovka, Ukraine | 3 | 87.1 ^{****} | ¹⁷ (Table 1) |
| Chernobyl | 8 | 284.6 ^{**} | ¹⁴ (Plate 60) |
| Gomel Region, Belarus | 30 | 480 | ¹⁸ (Fig. 2) |
| Outer area of Chernobyl and Gomel Region, Belarus | 100 | 22.8 ^{**} | ¹⁴ (Plate 60) |
| Belarus, Ukraine, Russia (low concentration areas) | - ^{*****} | 3.4 ^{**} , ^{****} | ¹⁶ (Figs. 3–5) |
| Austria | 1100 | 0.3 ^{**} | ¹⁵ |
| Sweden (low concentration areas) | 1250 | 0.3 ^{**} , ^{****} | ¹¹ (Fig. 1) |
| Sweden (high concentration areas) | 1250 | 1.0 ^{**} , ^{****} | ¹¹ (Fig. 1) |
| Greece | 1400 | 0.8 ^{***} | ¹² |

Table 1. Summary of soil ¹³⁷Cs concentrations contaminated by the FNPP and CNPP accidents. *For the FNPP accident, arithmetic mean was reported when more than one reference reported the soil concentration for the same location. Concentrations at top soil (0–10 cm) were presented. **A typical soil density of 1300 kg m⁻³ (²¹) and top 5 cm sampled surface soil^{11,17,30} were assumed. ***A typical soil density of 1300 kg m⁻³ (²¹) was assumed. ****Value corrected to 1 May 1986. *****See text.

to 7.6 mSv yr⁻¹ after 3 month of the FNPP accident. Comparing with our dose calculations, higher dose levels were expected for the estimations by Taira *et al.* since they included the contribution from ¹³⁴Cs radionuclides, which was higher (for example, the dose contribution of ¹³⁴Cs was 3 times higher than ¹³⁷Cs in the early period after the accident⁴⁷). For the same reason, our calculated dose of 3.6 mSv yr⁻¹ for the Minamisohma City was also comparable with that of 4.6 mSv yr⁻¹ at a nearby village – Iitate Village²⁶, to which ¹³⁴Cs and ¹³⁷Cs were the contributors. It is noted that the differences in dose levels could also be due to the adoption of different calculation methods. For instance, several empirical coefficients, such as occupancy-shielding factor, were adopted for the dose calculations for the work of Taira *et al.*

Regarding the accident in Ukraine, a recent study reported the external effective dose of 22 mSv yr⁻¹ in soil samples taken in CNPP (Manany)³⁰. The effective dose was calculated based on multiple radionuclides with predominated activity contribution from ¹³⁷Cs. Our ¹³⁷Cs dose calculation at the CNPP of 16 mSv yr⁻¹ (Fig. 1) was thus reasonably compared with the reported value. There were large variations in the estimated external effective doses reported in the literature in western Bryansk, Russia - an area with the most significant soil contamination in Russia. For instance, Ramzaev *et al.*²⁸ reported effective doses from 0.6 to 1.9 mSv yr⁻¹ but Thornberg *et al.*²⁷ reported values up to 2.8 mSv yr⁻¹. The large variations in the effective doses were reflected by the corresponding heterogeneity in soil activity concentrations from <45 kBq m⁻² to >1806 kBq m⁻²¹⁶. Nevertheless, our calculated effective dose for Russia in areas with low soil concentration (0.19 mSv yr⁻¹ in Fig. 1) was comparable to the minimum dose (0.6 mSv yr⁻¹) evaluated in these studies. Our result calculated for Gomel, Belarus (1.3 mSv yr⁻¹, Fig. 1) was comparable to the estimation by Thornberg *et al.* (2.8 mSv yr⁻¹)²⁷, with similar soil contamination levels (≤1806 kBq m⁻²) in both Gomel and Bryansk¹⁶. All values presented here are corrected to values as in 1986.

Methods

Calculation of the conversion coefficients. The conversion coefficients for different human organs irradiated by gamma photons from ¹³⁷Cs in soil were calculated by the MCNP5/X version 2.6.0 code⁴⁸. Detailed descriptions of the coefficients for different organs are available elsewhere (e.g. Krstić and Nikezić⁴⁹). Briefly, an Oak Ridge National Laboratory (ORNL) mathematical phantom described in ICRU Report 48⁵⁰ and Eckerman *et al.*⁵¹ was adopted for the absorbed dose calculations⁵². Similar methods have been used for dose calculations in many studies^{53–56}. The phantom consists of elliptical cylinders, truncated circular cones, circular cylinders, half ellipsoids, etc. to represent the trunk, arms, legs, feet, neck, head and female breasts. These “organs” were described by mathematical equations and inequalities⁵¹, which were then programmed in the input files for the MCNP code. Totally 66 (68) cells and 180 (188) surfaces were used for a male (female) phantom (Fig. 2). Transport of gamma photons with energy 662 keV from soil to target organs was simulated by the MCNP code. The soil source (pure SiO₂) was assumed to be cylindrical shape with a radius of 3 m. Photons emitted farther than 3 m from the phantom have small probability to hit the target and were neglected here. The ¹³⁷Cs vertical migration is known to be very slow and most of the accident-derived ¹³⁷Cs was found within the top 15 cm of the soil¹⁶. The profiles reported in IAEA¹⁶ in Ukraine and Taira *et al.*²⁶ in Iitate village, Japan were adopted respectively

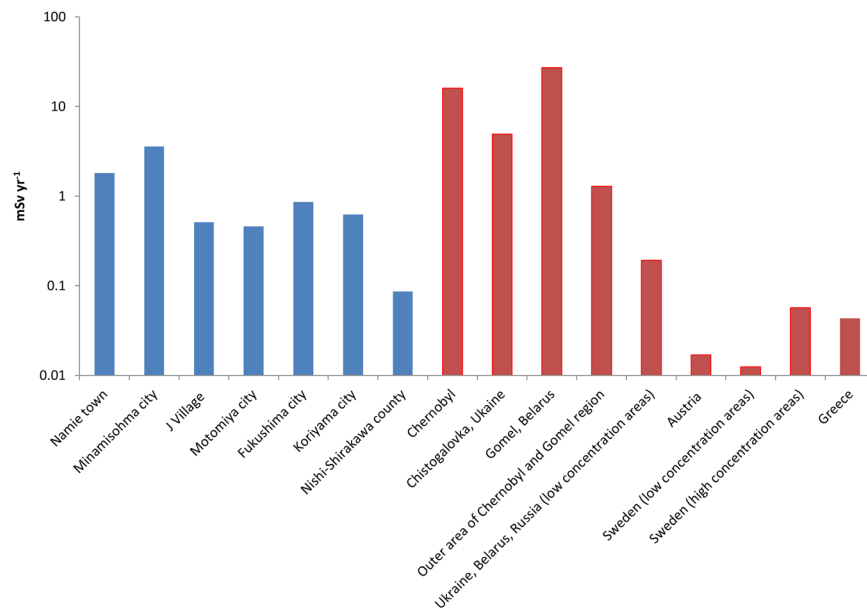


Figure 1. Comparison of external radiation doses from soil ¹³⁷Cs. Annual external effective dose (mSv yr⁻¹) calculated for various areas contaminated by the FNPP (blue) and CNPP (brown) accidents.

(Supplementary Materials S2) as the ¹³⁷Cs distribution in soil cylinder impacted by the CNPP and FNPP accidents in the current study despite the information of site-specific ¹³⁷Cs vertical profile in soil is not always available. The ¹³⁷Cs concentration for the top 5 cm soil was about twice as that for the next 5 cm soil for both profiles. The soil profile adopted here is consistent with those reported elsewhere^{57,58}. The cylinder representing the source was split into smaller cylinders 2 cm in height.

Homogenous distribution of the ¹³⁷Cs radionuclides in smaller cylinders were assumed and uniform sampling of initial points in these small cylinders was applied. Totally, 10⁸ simulations were run for each source to ensure small calculation uncertainties (relative error is less than 10%). The MCNP energy deposition tally F6 was used for dose estimation. Conversion of units was applied to the MCNP results to obtain the conversion coefficient (in fGy per Bq s kg⁻¹) for all major organs as a function of the source depth. The conversion coefficient is the absorbed dose rate in target organ per unit activity concentration in soil. The coefficient as a function of soil depth, which has been previously presented⁴⁹, is given in Supplementary Materials S3.

Calculation of the effective dose due to soil contamination from FNPP and CNPP accidents.

The equivalent dose (H_t) in a tissue or organ (t) was calculated through the sum:

$$H_t = \sum_r w_r D_{t,r} \quad (1)$$

where $D_{t,r}$ is the dose absorbed in that organ from ¹³⁷Cs in soil for 1 year (in Gy y⁻¹) from the radiation of type r ; the radiation weighting factor is $w_r = 1$ for photons of all energies according to ICRP Publication 60³¹. The soil concentrations of ¹³⁷Cs were obtained from Table 1 below. Contributions to the equivalent dose in organs from a soil layer were calculated by multiplying the above conversion coefficients with the number of disintegrations occurring during one year. The contributions from different layers were then summed up to obtain the equivalent dose in that organ.

The effective dose (E) for an individual standing on the ground was calculated according to ICRP Publication 116⁵⁹:

$$E = \sum_t w_t (H_{t,male} + H_{t,female})/2 \quad (2)$$

where $H_{t,male}$ and $H_{t,female}$ are equivalent doses in male and female phantoms, respectively. The values of w_t are given in ICRP Publication 103⁶⁰. An average outdoor occupancy factor of 0.3^{61,62} was included to the annual effective dose calculation. The factor used is comparable to the UNSCEAR's value of 0.2, which is suggested to have differences around the world⁶³. The differences are due to that, for instance, human is considered likely to spend more (less) time indoors for industrialized (agricultural) countries in temperate (warm) climates. More details of the occupancy factor could be referred to Hinrichsen *et al.*⁶⁴ It is noted that the external dose is likely to be changed when the radionuclides migrate deeper into the soil⁶⁴.

Compilation of soil ¹³⁷Cs concentration. The soil sample data were extracted from various references available in the literature as shown in Table 1. Concentrations in the top soil (0–10 cm) were presented. The

| Location | Bone surface | Bone Marrow | Skin | Ovaries | Testes | Gonads | Breast | Lung | Thyroid | Liver | Bladder | Colon | Stomach | Esophagus | Remainder |
|--|--------------|-------------|--------|---------|--------|--------|--------|-------|---------|-------|---------|-------|---------|-----------|-----------|
| FNPP accident | | | | | | | | | | | | | | | |
| Namie town | 23000 | 6400 | 49000 | 1000 | 10000 | 5700 | 3200 | 2400 | 790 | 4300 | 6100 | 4400 | 3500 | 1700 | 8100 |
| Minamisohma city | 46000 | 13000 | 99000 | 2000 | 20000 | 11000 | 6400 | 4800 | 1600 | 8500 | 12000 | 8700 | 6900 | 3400 | 16000 |
| J Village | 6600 | 1800 | 14000 | 290 | 2900 | 1600 | 920 | 690 | 220 | 1200 | 1700 | 1200 | 1000 | 490 | 2300 |
| Motomiya city | 5900 | 1600 | 13000 | 260 | 2600 | 1400 | 820 | 620 | 200 | 1100 | 1500 | 1100 | 890 | 440 | 2100 |
| Fukushima city | 11000 | 3000 | 24000 | 480 | 4900 | 2700 | 1500 | 1200 | 380 | 2000 | 2900 | 2100 | 1700 | 830 | 3900 |
| Koriyama city | 8000 | 2200 | 17000 | 350 | 3600 | 2000 | 1100 | 840 | 270 | 1500 | 2100 | 1500 | 1200 | 600 | 2800 |
| Nishi-Shirakawa county | 1100 | 300 | 2400 | 48 | 500 | 270 | 160 | 120 | 38 | 210 | 290 | 210 | 170 | 83 | 390 |
| CNPP accident | | | | | | | | | | | | | | | |
| Chernobyl | 210000 | 57000 | 430000 | 8900 | 92000 | 51000 | 29000 | 22000 | 7000 | 38000 | 54000 | 39000 | 31000 | 15000 | 72000 |
| Chistogalovka, Ukraine | 63000 | 17000 | 130000 | 2700 | 28000 | 15000 | 8900 | 6700 | 2100 | 12000 | 17000 | 12000 | 9600 | 4700 | 22000 |
| Gomel, Belarus | 350000 | 96000 | 730000 | 15000 | 160000 | 85000 | 49000 | 37000 | 12000 | 64000 | 91000 | 66000 | 53000 | 26000 | 120000 |
| Outer areas of Chernobyl and Gomel Region, Belarus | 17000 | 4600 | 35000 | 720 | 7400 | 4100 | 2300 | 1700 | 560 | 3100 | 4300 | 3100 | 2500 | 1200 | 5700 |
| Ukraine, Belarus, Russia with relatively low ¹³⁷ Cs concentration (2.8 kBq kg ⁻¹) | 2500 | 680 | 5200 | 110 | 1100 | 610 | 350 | 260 | 84 | 460 | 650 | 470 | 380 | 190 | 860 |
| Austria | 220 | 60 | 460 | 9.4 | 97 | 53 | 31 | 23 | 7.4 | 40 | 57 | 41 | 33 | 16 | 75 |
| Sweden (low concentration areas) | 160 | 40 | 330 | 6.9 | 72 | 39 | 22 | 17 | 5.5 | 30 | 42 | 30 | 24 | 12 | 55 |
| Sweden (high concentration areas) | 730 | 200 | 1500 | 32 | 330 | 180 | 100 | 77 | 25 | 140 | 190 | 140 | 110 | 55 | 250 |
| Greece | 560 | 150 | 1200 | 24 | 250 | 140 | 79 | 59 | 19 | 100 | 150 | 110 | 85 | 42 | 190 |

Table 2. Calculated equivalent doses ($\mu\text{Sv yr}^{-1}$) in organs due to external dose from soil in various areas contaminated by the NPP accidents.

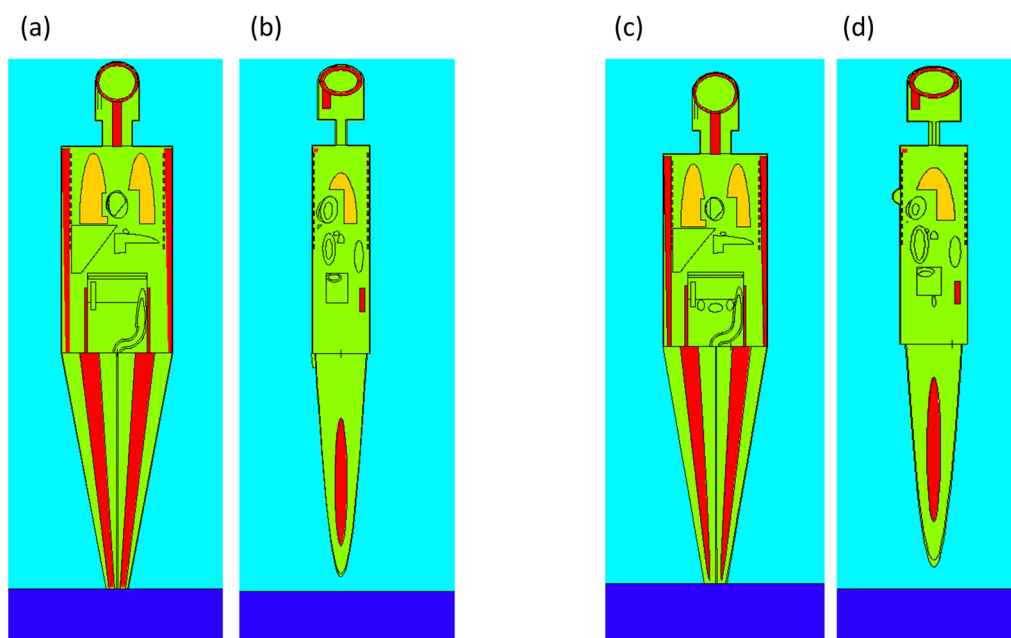


Figure 2. Mathematical phantoms output from the MCNPX code. (a) male (front-view); (b) male (side-view); (c) female (front-view); and (d) female (side-view).

mean concentrations were preferred. In case that the mean concentration was not available and there was a large variation of the concentration within a large area (e.g. Sweden), both lower- and higher-end concentrations were reported. For the data relevant to the FNPP accident, arithmetic means were reported when more than one reference reported the soil concentration for the same location. The data relevant to the CNPP accident were usually reported as kBq m^{-2} . A typical soil density of 1300 kg m^{-3} ⁽²¹⁾ and top 5 cm sampled surface soil^{11,17,30} were assumed if these information were not available.

Concluding remarks

Our study summarized the literature values of ^{137}Cs soil concentrations influenced by the CNPP and FNPP and rationalized their spatial distributions. The soil distributions were affected by the location of NPPs (either inland or coastal), initial release heights and emission strengths of the contaminants, as well as the atmospheric transport pathways. We then used these values and the conversion coefficients determined by the MCNP code to calculate the organs doses ($\mu\text{Sv yr}^{-1}$) due to ^{137}Cs in soil in various areas contaminated by the NPP accidents, which are important for cancer risk assessment but were seldom reported. Finally, we discussed the similarity and differences of our calculated effective doses with values reported in the literature. Given the available soil concentrations of ^{137}Cs , the annual effective doses at various locations could be calculated, where estimations of the effective doses at these locations were not available.

Received: 28 October 2019; Accepted: 21 April 2020;

Published online: 13 May 2020

References

- Pöllänen, R., Valkama, I. & Toivonen, H. Transport of radioactive particles from the Chernobyl accident. *Atmos. Environ.* **31**, 3575–3590 (1997).
- Persson, C., Rodhe, H. & Geer, L. E. D. The Chernobyl accident—a meteorological analysis of how radionuclides reached and were deposited in Sweden. *Ambio* **16**, 20–31 (1987).
- Wheeler, D. A. Atmospheric dispersal and deposition of radioactive material from Chernobyl. *Atmos. Environ.* **22**, 853–863 (1988).
- Puhakka, T., Jylhä, K., Saarikivi, P., Koistinen, J. & Koivuokoski, J. Meteorological factors influencing the radioactive deposition in Finland after the Chernobyl accident. *J. Applied Meteor.* **29**, 813–829 (1990).
- Stohl, A. *et al.* Xenon-133 and caesium-137 releases into the atmosphere from the Fukushima Daiichi nuclear power plant: determination of the source term, atmospheric dispersion, and deposition. *Atmos. Chem. Phys.* **12**, 2313–2343 (2012).
- Draxler, R. R. & Rolph, G. D. Evaluation of the Transfer Coefficient Matrix (TCM) approach to model the atmospheric radionuclide air concentrations from Fukushima. *J. Geophys. Res.* **117**, D05107 (2012).
- Ten Hoeve, J. E. & Jacobson, M. Z. Worldwide health effects of the Fukushima Daiichi nuclear accident. *Energy Environ. Sci.* **5**, 8743–8757 (2012).
- Wai, K. M. & Yu, P. K. N. Trans-oceanic transport of ^{137}Cs from the Fukushima nuclear accident and impact of hypothetical Fukushima-like events of future nuclear plants in Southern China. *Sci. Total Environ.* **508**, 128–135 (2015).
- Masson, O. *et al.* Tracking of airborne radionuclides from the damaged Fukushima Daiichi nuclear reactors by European networks. *Environ. Sci. Technol.* **45**, 7670–7677 (2011).
- Thakur, P., Ballard, S. & Nelson, R. An overview of Fukushima radionuclides measured in the northern hemisphere. *Sci. Total Environ.* **458–460**, 577–613 (2013).
- Rosén, K., Andersson, I. & Lönsjö, H. Transfer of radiocaesium from soil to vegetation and to grazing lambs in a mountain area in northern Sweden. *J. Environ. Radioact.* **26**, 237–257 (1995).
- Petropoulos, N. P., Hinis, E. P. & Simopoulos, S. E. ^{137}Cs Chernobyl fallout in Greece and its associated radiological impact. *Environ. Int.* **22**, 369–373 (1996).
- Krstić, D., Nikezić, D. & Bek-Uzarov, D. J. Effective dose estimation for the population in Kragujevac due to the Chernobyl accident. *J. Environ. Radioact.* **34**, 253–266 (1997).
- De Cort, M., *et al.* Atlas of cesium deposition on Europe after the Chernobyl accident. EUR Report Nr. 16733. (Brussels-Luxemburg: Office for Official Publications of the European Communities, ECSC-EEC-EAEC, 1998).
- Bossew, P. *et al.* Contamination of Austrian soil with caesium-137. *J. Environ. Radioact.* **55**, 187–194 (2001).
- IAEA. Present and future environmental impact of the Chernobyl accident (International Atomic Energy Agency, Austria, 2001).
- Malek, M. A., Hinton, T. G. & Webb, S. B. A comparison of ^{90}Sr and ^{137}Cs uptake in plants via three pathways at two Chernobyl-contaminated sites. *J. Environ. Radioact.* **58**, 129–141 (2002).
- Mašmova, S. Radiation effects on the populations of soil invertebrates in Belarus in Equidosisimetry – Ecological standardization and equidosisimetry for radioecology and environmental ecology (eds Bréchnignac, F. & Desmet, G.) Proceedings of the NATO Advanced Research Workshop (Ukraine, 2002).
- Krstić, D., Nikezić, D., Stevanovic, N. & Jelić, M. Vertical profile of ^{137}Cs in soil. *Appl. Radiat. Isot.* **61**, 1487–1492 (2004).
- Tagami, K. *et al.* Specific activity and activity ratios of radionuclides in soil collected about 20 km from the Fukushima Daiichi Nuclear Power Plant: Radionuclide release to the south and southwest. *Sci. Total Environ.* **409**, 4885–4888 (2011).
- Yasunari, T. J. *et al.* Cesium-137 deposition and contamination of Japanese soils due to the Fukushima nuclear accident. *PNAS* **108**, 19530–19534 (2011).
- Tanaka, K. *et al.* Vertical profiles of Iodine-131 and Cesium-137 in soils in Fukushima Prefecture related to the Fukushima Daiichi Nuclear Power Station Accident. *Geochem. J.* **46**, 73–76 (2012).
- Tazoe, H. *et al.* Radioactive pollution from Fukushima Daiichi nuclear power plant in the terrestrial environment. *Radiat. Prot. Dosim.* **152**, 198–203 (2012).
- Yang, G., Tazoe, H. & Yamada, M. ^{135}Cs activity and $^{135}\text{Cs}/^{137}\text{Cs}$ atom ratio in environmental samples before and after the Fukushima Daiichi Nuclear Power Plant accident. *Sci. Rep.* **6**, 24119 (2016).
- Yoshida, M. & Suzuki, T. Environmental radiation measurements immediately after the accident and dose evaluations based on soil deposition. Proceedings of the International Symposium on Environmental monitoring and dose estimation of residents after accident of TEPCO's Fukushima Daiichi Nuclear Power Stations. Kyoto University, Kyoto, Japan http://www.rri.kyoto-u.ac.jp/anzen_kiban/outcome/index.html (2012).
- Taira, Y. *et al.* Environmental contamination and external radiation dose rates from radionuclides released from the Fukushima Nuclear Power Plant. *Radiat. Prot. Dosim.* **151**, 537–545 (2012).
- Thornberg, C. *et al.* External and internal irradiation of a rural Bryansk (Russia) population from 1990 to 2000, following high deposition of radioactive caesium from the Chernobyl accident. *Radiat Environ Biophys.* **44**, 97–106 (2005).
- Ramzaev, V. *et al.* Gamma-dose rates from terrestrial and Chernobyl radionuclides inside and outside settlements in the Bryansk Region, Russia in 1996–2003. *J. Environ. Radioact.* **85**, 205–227 (2006).
- Ramzaev, V., Botter-Jensen, L., Thomsen, K. J., Andersson, K. G. & Murray, A. S. An assessment of cumulative external doses from Chernobyl fallout for a forested area in Russia using the optically stimulated luminescence from quartz inclusions in bricks. *J. Environ. Radioact.* **99**, 1154–1164 (2008).
- Taira, Y. *et al.* Vertical distribution and estimated doses from artificial radionuclides in soil samples around the Chernobyl Nuclear Power Plant and the Semipalatinsk Nuclear Testing Site. *PLoS One* **8**, e57524 (2013).
- ICRP. Recommendations of the International Commission on Radiological Protection - ICRP Publication 60 (Oxford, Pergamon Press, 1991).
- Gao, Y. *et al.* A comparison of pediatric and adult CT organ dose estimation methods. *BMC Med Imaging* **17**, 28 (2017).

33. Tian, X. *et al.* Pediatric chest and abdominopelvic CT: organ dose estimation based on 42 patient models. *Radiology* **270**, 535–547 (2014).
34. National Research Council. Analysis of Cancer Risks in Populations Near Nuclear Facilities: Phase 1. (The National Academies Press, Washington, DC, 2012).
35. Kawamura, H. *et al.* Preliminary Numerical Experiments on Oceanic Dispersion of ¹³¹I and ¹³⁷Cs Discharged into the Ocean because of the Fukushima Daiichi Nuclear Power Plant Disaster. *J. Nucl. Sci. Technol.* **48**, 1349–1356 (2011).
36. Morino, Y., Ohara, T. & Nishizawa, M. Atmospheric behavior, deposition, and budget of radioactive materials from the Fukushima Daiichi nuclear power plant in March 2011. *Geophys. Res. Lett.* **38**, L00G11 (2011).
37. Hass, H. *et al.* Simulation of the Chernobyl radioactive cloud over Europe using the EURAD model. *Atmos. Environ.* **24**, 673–692 (1990).
38. Suh, K. S., Han, M. H., Jung, S. H. & Lee, C. W. Numerical simulation for a long-range dispersion of a pollutant using Chernobyl data. *Math. Comput. Model.* **49**, 337–343 (2009).
39. Anspaugh, L. R., Catlin, R. J. & Goldman, M. The global impact of the Chernobyl reactor accident. *Science* **242**, 1513–1519 (1988).
40. Dreicer, M. *et al.* Consequences of the Chernobyl accident for the natural and human environments in One decade after Chernobyl: summing up the consequences of the accident (eds. EC, IAEA & WHO) 319–361 (IAEA, 1996).
41. UNSCEAR. Sources and effects of ionizing radiation (annex D). United Nation Scientific Committee on the Effects of Atomic Radiation. United Nation Scientific Committee on the Effects of Atomic Radiation to the General Assembly (New York: United Nations, 2008).
42. Hamada, N. & Ogino, H. Food safety regulations: what we learned from the Fukushima nuclear accident. *J. Environ. Radioact.* **111**, 83–99 (2012).
43. Winiarek, V., Bocquet, M., Saunier, O. & Mathieu, A. Estimation of errors in the inverse modeling of accidental release of atmospheric pollutant: Application to the reconstruction of the cesium-137 and iodine-131 source terms from the Fukushima Daiichi power plant. *J. Geophys. Res.* **117**, D05122 (2012).
44. Kobayashi, T., Nagai, H., Chino, M. & Kawamura, H. Source term estimation of atmospheric release due to the Fukushima Daiichi Nuclear Power Plant accident by atmospheric and oceanic dispersion simulations. *J. Nucl. Sci. Technol.* **50**, 255–264 (2013).
45. Karunakara, N. *et al.* ¹³⁷Cs concentration in the environment of Kaiga of south west coast of India. *Health Phys.* **81**, 148–155 (2001).
46. Tahir, S. N., Jamil, K., Zaidi, J. H., Arif, M. & Ahmed, N. Activity Concentration of ¹³⁷Cs in soil samples from Punjab province (Pakistan) and estimation of gamma-ray dose rate for external exposure. *Radiat. Prot. Dosim.* **118**, 345–351 (2006).
47. Tsubokura, M. *et al.* Individual external doses below the lowest reference level of 1 mSv per year five years after the 2011 Fukushima nuclear accident among all children in Soma City, Fukushima: A retrospective observational study. *PLoS One* **12**, e0172305 (2017).
48. Monte Carlo Team. MCNP – a General Monte Carlo N-Particle Transport Code, Version 5 Vol. I: Overview and Theory (Los Alamos National Laboratory, 2003).
49. Krstić, D. & Nikezić, D. External doses in humans from ¹³⁷Cs in soil. *Health Phys.* **91**, 249–257 (2006).
50. ICRU. Phantoms and computational models in therapy, diagnostics and protection - ICRU Report 48 (Bethesda MD, 1992).
51. Eckerman, K. F., Cristy, M. & Ryman, J. C. The ORNL mathematical phantom series (Oak Ridge National Laboratory, 1996).
52. Krstić, D. & Nikezić, D. Input files with ORNL-mathematical phantoms of the human body for MCNP-4B. *Comput. Phys. Commun.* **176**, 33–37 (2007).
53. Zankl, M., Petoussi, N. & Drexler, G. Effective dose and effective dose equivalent—the impact of the new ICRP definition for external photon irradiation. *Health Phys.* **62**, 385–399 (1992).
54. Yamaguchi, Y. Age-dependent effective dose for external photons. *Radiat. Prot. Dosim.* **55**, 123–129 (1994).
55. Bhati, S., Sharma, R. C. & Raj, V. V. Assessing skull burdens of actinides using a mathematical phantom: a Monte Carlo approach. *Radiat. Prot. Dosim.* **103**, 247–254 (2003).
56. Chou, D. P., Wang, J. N. & Chen, I. J. Age-dependent protection quantities for external neutron irradiation. *Radiat. Prot. Dosim.* **104**, 5–16 (2003).
57. Östlund, K., Samuelsson, C., Mattsson, S. & Rääf, C. L. The influence of ¹³⁴Cs on the ¹³⁷Cs gamma-spectrometric peak-to-valley ratio and improvement of the peak-to-valley method by limiting the detector field of view. *Appl. Radiat. Isot.* **128**, 249–255 (2017).
58. Malins, A. *et al.* Evaluation of ambient dose equivalent rates influenced by vertical and horizontal distribution of radioactive cesium in soil in Fukushima Prefecture. *J. Environ. Radioact.* **151**, 38–49 (2016).
59. ICRP. Conversion Coefficients for Radiological Protection Quantities for External Radiation Exposures. Ann. ICRP 40, 2-5, ICRP Publication 116 (2010).
60. ICRP. The 2007 Recommendations of the International Commission on Radiological Protection - ICRP Publication 103 (Oxford, Pergamon Press, 2007).
61. Nair, R. R. *et al.* Background radiation and cancer incidence in Kerala, India-Karanagappally cohort study. *Health Phys.* **96**, 55–66 (2009).
62. Yu, C. & LePoire, D. Dose and Risk Assessment. Argonne National Laboratory, USA. https://www.iaea.org/OurWork/ST/NE/NEFW/documents/ENVIRONET/TM_ER_Radiologically_Contaminate_Sites_ANL/D3/Dose_and_Risk_Assessment.pdf (2010).
63. UNSCEAR. Sources and effects of ionizing radiation – Volume I: Sources. United Nation Scientific Committee on the Effects of Atomic Radiation. United Nation Scientific Committee on the Effects of Atomic Radiation to the General Assembly with Scientific Annexes (New York: United Nations, 2000).
64. Hinrichsen, Y., Finck, R., Martinsson, J., Rääf, C. & Andersson, K. G. Influence of the migration of radioactive contaminants in soil, resident occupancy, and variability in contamination on isodose lines for typical Northern European houses. *Sci. Rep.* **9**, 7876 (2019).

Acknowledgements

We acknowledge the US Geological Survey for the provision of free access of the LandSat data from their website. We also acknowledge Mr. Sheng-Kai Zeng at the Graduate Institute of Space Science, National Central University, Taiwan for his contribution to prepare the satellite images for early submission.

Author contributions

K.M.W. and K.N.Y. designed the research. K.M.W. and D.K. modified the computer codes, K.M.W. performed the research, implemented the codes, analyzed the data and wrote the manuscript. T.H.L. prepared the satellite images. K.N.Y., D. K., D.N. and T.H.L. reviewed and modified the manuscript.

Competing interests

The authors declare no competing interests.

Additional information

Supplementary information is available for this paper at <https://doi.org/10.1038/s41598-020-64812-9>.

Correspondence and requests for materials should be addressed to K.-M.W. or P.K.N.Y.

Reprints and permissions information is available at www.nature.com/reprints.

Publisher's note Springer Nature remains neutral with regard to jurisdictional claims in published maps and institutional affiliations.



Open Access This article is licensed under a Creative Commons Attribution 4.0 International License, which permits use, sharing, adaptation, distribution and reproduction in any medium or format, as long as you give appropriate credit to the original author(s) and the source, provide a link to the Creative Commons license, and indicate if changes were made. The images or other third party material in this article are included in the article's Creative Commons license, unless indicated otherwise in a credit line to the material. If material is not included in the article's Creative Commons license and your intended use is not permitted by statutory regulation or exceeds the permitted use, you will need to obtain permission directly from the copyright holder. To view a copy of this license, visit <http://creativecommons.org/licenses/by/4.0/>.

© The Author(s) 2020